Chapter 1
Crystal Bonding

Abstract The bonding of atoms is described as function of the electrostatic forces, covalent bonding, mixed bonding van der Waals bonding hydrogen and metallic bonding, and Born repulsion, yielding equilibrium distance and ionic or atomic radii that are tabulated. Repulsive potential softness parameters and Mohs hardness are tabulated Close packing of ions/atoms determine ordering preferences. Compressibility and Madelung constants, lattice constants and bond length are discussed and tabulated (Table 1.2). Electronegativity, ionicity and effective charges for numerous AB-compounds are listed. Atomic electron density profiles are given.

The bonding of atoms in semiconductors has primary influence of forming the lattice of any solar cell and is accomplished by electrostatic forces and by the tendency of atoms to fill their outer shells. Interatomic attraction is balanced by short-range repulsion due to strong resistance of atoms against interpenetration of core shells. The knowledge of the detail of this interaction is not only of help for selecting most appropriate materials for solar cells but also for judging about the ease of incorporation of desirable crystal defects and avoiding others.

The different types of the bonding of condensed matter (solids) will be reviewed, irrespective of whether they are crystalline or amorphous.

The formation of solids is determined by the interatomic forces and the size of the atoms shaping the crystal lattice. The interatomic forces are composed of a far-reaching attractive and a short-range repulsive component, resulting in an *equilibrium distance* of vanishing forces at an interatomic distance r_e, at which the potential energy shows a minimum (Fig. 1.1). In Binary compounds, this equilibrium distance r_e can be written as the sum of *atomic radii*

$$r_e = r_A + r_B, \tag{1.1}$$

where r_A and r_B are characteristic for the two atoms A and B (Fig. 1.2).

Attractive interatomic forces are predominantly *electrostatic* (e.g., in ionic, metallic, van der Waals, and hydrogen bonding) or are a consequence of sharing valence electrons to fill their outer shells, resulting in *covalent* bonding. Most materials show *mixed bonding*, i.e., at least two of these bond types contribute significantly

K.W. Böer, *Handbook of the Physics of Thin-Film Solar Cells*,
DOI 10.1007/978-3-642-36748-9_1,

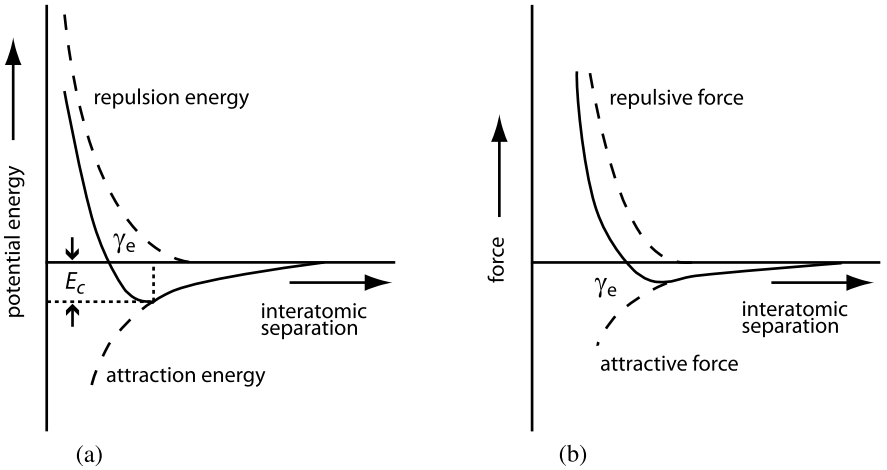

Fig. 1.1 Interaction potential (**a**) and forces (**b**) between two atoms; r_e is the equilibrium distance; E_c is the bonding energy at $r = r_e$

to the interatomic interaction. In the better compound semiconductors, the mixed bonding is more covalent and less ionic. In other semiconductors, one of the other types of bonding may contribute, e.g., van der Waals bonding in organic crystals, and metallic bonding in highly conductive semiconductors.

The *repulsive interatomic* forces, called Born forces (see Born and Huang 1954), are caused by a strong resistance of the electronic shells of atoms against interpenetration. The repulsive Born potential is usually modeled with a strong power law[1]

$$eV(r) = \frac{\beta}{r^m} \quad \text{with } m \simeq 10, \ldots, 12. \tag{1.3}$$

1.1 Ionic Bonding

Ionic bonding is caused by Coulomb attraction between ions. Such ions are formed by the tendency of atoms to complete their outer shells. This is most easily accomplished by compounds between elements of group I and group VII of the periodic system of elements; here one electron needs to be exchanged. The bonding is then described by isotropic (radial-symmetric) *nonsaturable* Coulomb forces attracting

[1] A better fit for the Born repulsion is obtained by the sum of a power and an exponential law:

$$V_{\text{Born}} = \frac{\beta}{r^m} + \gamma \exp\left(-\frac{r}{r_0}\right). \tag{1.2}$$

r_0 is the *softness parameter*, listed for ions in Table 1.7. For more sophisticated repulsion potentials, see Shanker and Kumar (1987). β is the force constant (see Eq. (1.1)) and m is an empirical exponent. For ionic crystals the exponent m lies between 6 and 10.

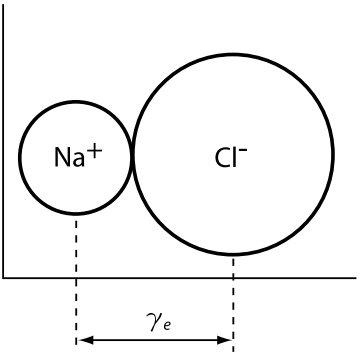

Fig. 1.2 Na^+ anion and Cl^- cation shown as hard spheres in actual ratio of radii

as many Na^+ ions as space permits around each Cl^- ion, and vice versa, while maintaining overall neutrality. This results in a closely packed NaCl lattice with a *coordination number* 6 (= number of nearest neighbors).

The energy gain between two ions can be calculated from the potential equation

$$eV = -\frac{e^2}{4\pi\varepsilon_0 r} + \frac{\beta}{r^m} \quad \text{for } r = r_e, \tag{1.4}$$

containing Coulomb attraction and Born repulsion. For an equilibrium distance $r_e = r_{Na^+} + r_{Cl^-} = 2.8$ Å results[2] in a minimum of the potential energy of $eV_{\min} \sim -5$ eV for a typical value of $m = 9$.

In a crystal we must consider *all* neighbors. For example, in an NaCl lattice, six nearest neighbors exert Coulomb attraction in addition to 12 next-nearest neighbors of equal charge exerting Coulomb repulsion, etc. This alternating interaction results in a summation that can be expressed by a proportionality factor A in the Coulomb term of Eq. (1.4), the *Madelung constant* (Madelung 1918).

For the NaCl crystal structure it follows

$$A = \frac{6}{\sqrt{1}} - \frac{12}{\sqrt{2}} + \frac{8}{\sqrt{3}} - \frac{6}{\sqrt{4}} + \frac{25}{\sqrt{5}} - \cdots + \cdots, \tag{1.5}$$

where each term presents the number of equidistant neighbors in the numerator and the corresponding distance (in lattice units) in the denominator. This series is only slowly converging. Ewald's method (the theta-function method) is powerful and facilitates the numerical evaluation of A. For NaCl, we obtain from (Madelung 1918; Born and Lande 1918):

$$eV = -A\frac{e^2}{4\pi\varepsilon_0 r_e} + \frac{\beta'}{r_e^m} \tag{1.6}$$

with $A = 1.7476$, a lattice binding energy of $eV_{\min}^A = H^0(\text{NaCl}) = 7.948$ eV, compared to an experimental value of 7.934 eV. Here β' and m are empirically obtained

[2] β can be eliminated from the minimum condition $\{dV/dr|_{r_e} = 0\}$. One obtains $\beta = e^2 r_e^{m-1}/(4\pi\varepsilon_0 m)$ and as cohesive energy $eV_{\min} = -e^2(m-1)/(4\pi\varepsilon_0 m_{r_e})$.

Table 1.1 Madelung constant for a number of crystal structures

Crystal structure	Madelung constant
NaCl	1.7476
CsCl	1.7627
Zinc-blende	1.6381
Wurtzite	1.6410
CaF_2	5.0388
Cu_2O	4.1155
TiO_2 (Rutile)	4.8160

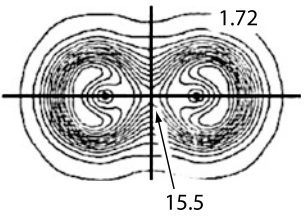

Fig. 1.3 Total charge contour plot of the O_2 molecule (after Cotton and Wilkinson 1979). Copyright Pergamon Press

from the observed lattice constant and compressibility. The Madelung constant is listed for several AB-compounds in Table 1.1 (see Sherman 1932).

The Born-Haber cycle is an empirical process of obtaining the lattice energy, i.e., the binding energy per mole. The process starts with the solid metal and gaseous halogen, and adds the heat of sublimation $W_{\text{subl}}(\text{Na})$ and the dissociation energy $(1/2)W_{\text{diss}}(\text{Cl})$; it further adds the ionization energy $W_{\text{ion}}(\text{Na})$ and the electron affinity $W_{\text{elaff}}(\text{Cl})$ in order to obtain a diluted gas of Na^+ and Cl^- ions; all of these energies can be obtained experimentally. These ions can be brought together from infinity to form the NaCl crystal by gaining the unknown lattice energy H^0 (NaCl). This entire sum of processes must equal the heat of formation W^0 (NaCl) which can be determined experimentally (Born 1919; Haber 1919):

$$W^0_{\text{solid}}(\text{NaCl}) = \left\{ W_{\text{subl}}(\text{Na}) + W_{\text{ion}}(\text{Na}) + \frac{1}{2} W_{\text{diss}}(\text{Cl}_2) + W_{\text{elaff}}(\text{Cl}) \right\} + H^0(\text{NaCl}). \tag{1.7}$$

A minor correction of an isothermal compression of NaCl from $p = 0$ to $p = 1$ (atm), heating it from $T = 0$ K to room temperature, and an adiabatic expansion of the ion gases to $p = 0$ has been neglected. The corresponding energies almost cancel. The error is <1 %.

1.2 Covalent Bonding

Covalent bonding is caused by two electrons that are shared between two atoms: they form an *electron bridge* as shown in Fig. 1.3 for a diatomic oxygen molecule. This bridge formation can be understood quantum-mechanically by a nonspherical

Table 1.2 Lattice constants (a in Å) and ratio of lattice constants c/a for simple predominantly ionic AB compounds (after Weissmantel and Hamann 1979)[a]

NaCl		Structure		CsCl Structure		Zinc-blende		Wurtzite		c/a
AgF	4.93	NaBr	5.973	BaS	6.363	AlP	5.431	AgI	4.589	1.63
AgCl	5.558	NaCl	6.433	CsCl	4.118	AlAs	5.631	AlN	3.110	1.60
AgBr	5.78	PbS	5.935	CsBr	4.296	AlSb	6.142	BeO	2.700	1.63
BaO	5.534	PbSe	6.152	CsI	4.571	BeS	4.86	CdS	4.139	1.62
BaS	6.363	PbTe	6.353	TiI	4.206	BeSe	5.08	CdSe	4.309	1.63
BaSe	6.633	RbF	5.651	TICI	3.842	BeTe	5.551	GaN	3.186	1.62
BaTe	7.000	RbCl	6.553	TiBr	3.978	CSi	4.357	InN	3.540	1.61
CaO	4.807	RbBr	6.868	TiI	4.198	CdS	5.832	MgTe	4.529	1.62
CaS	5.69	RbI	7.341	NH_4Cl	3.874	CdSe	6.052	MnS	3.984	1.62
CaSe	5.992	SnAs	5.692	NH_4Br	4.055	CdTe	6.423	MnSc	4.128	1.63
CaTe	6.358	SnTe	6.298	NH_4I	4.379	CuF	4.264	TaN	3.056	–
CdO	4.698	SrO	5.156	$TiNO_3$	4.31	CuCl	5.417	ZnO	3.249	1.60
KF	5.351	SrS	5.582	CsCN	4.25	CuBr	5.091	ZnS	3.819	1.64
KCl	6.283	SrSe	6.022			GaP	5.447	NH_4F	4.399	1.60
KBr	6.599	SrTe	6.483			GaAs	5.646			
KI	7.066	TaC	4.454			GaSb	6.130			
LiF	4.025	TiC	4.329			HgSe	6.082			
LiCl	5.140	TiN	4.244			HgTe	6.373			
LiBr	5.501	TiO	4.244			InAs	6.018			
LiI	6.012	VC	4.158			InSb	6.474			
MgO	4.211	VN	4.137			MnS	5.611			
MgS	5.200	VO	4.108			MnSe	5.832			
MgSe	5.462	ZrC	4.696			ZnS	5.423			
NaF	4.629	ZrN	4.619			ZnSe	5.661			
NaCl	5.693					ZnTe	6.082			

[a]For explanation of the different crystal structures see Chap. 2

electron density distribution extending between the bonded atoms. Examples of such density distributions are shown in Fig. 1.3 for an O_2 molecule and schematically in Fig. 1.4 for a molecule formation with electrons in a $1s$ or $2p$ state, e.g., for H_2 or F_2, respectively.

If an approaching atom of the same element has in its protruding part of the electron density distribution an unpaired electron with antiparallel spin, both eigenfunctions may overlap; the Pauli principle is not violated.

Their combined wave function ($\Psi_+ = \Psi_A + \Psi_B$) yields an increased electron density Ψ^2 in the overlap region (see Fig. 1.5a); the result is an *attractive force* between these two atoms *in the direction of the overlapping eigenfunctions*. This is the state of lowest energy of the two atoms, the *bonding state*.

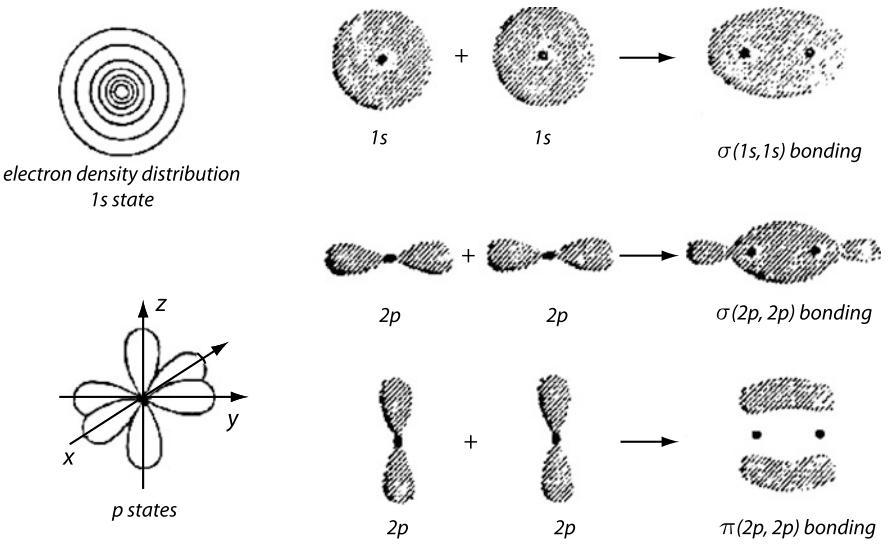

Fig. 1.4 Atomic and molecular electron density distribution for $\sigma(s)$, $\sigma(p)$, and $\pi(p)$ bonding—see Weissmantel and Hamann (1979)

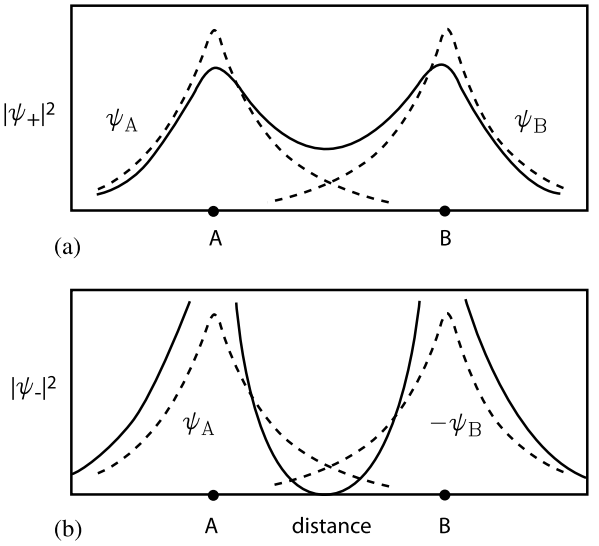

Fig. 1.5 Wavefunctions of one-electron states [*dashed curves*—identical in (**a**) and (**b**)] and probability function to find one electron (*solid curves*) in (**a**), a bonding state, and (**b**), an antibonding state, showing finite and vanishing electron density at the center between atoms A and B for these two states, respectively [observe the plotting of $-\psi_B$ in (**b**)]. The picture of these two one-electron states shown here shall not be confused with the two-electron potential given in Fig. 1.6

There is also a state of higher energy, the *antibonding state*, with $\Psi_- = \Psi_A - \Psi_B$ in which the spin of both electrons is parallel. Here the electrons are repulsed because of the Pauli principle, and the electron clouds cannot penetrate each other; the electron density between both atoms vanishes (Fig. 1.5b). The resulting potential distribution as a function of the interatomic distance between two hydrogen atoms forming an H_2 molecule is given in Fig. 1.6, with both the bonding

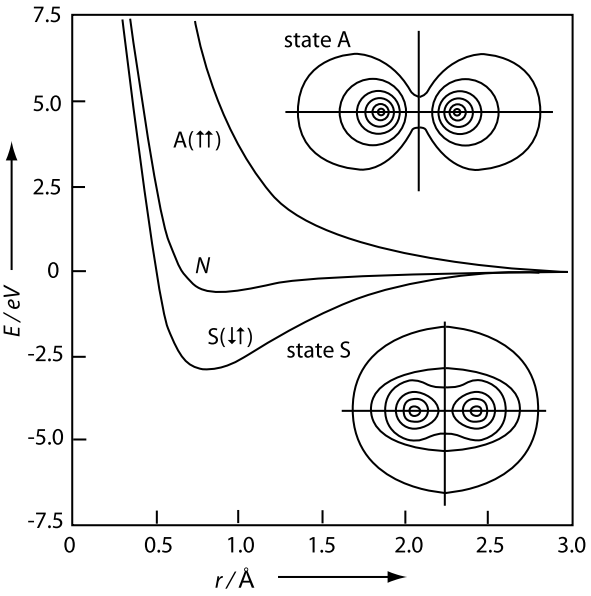

Fig. 1.6 Potential energy for the two valence electrons of two covalently bound hydrogen atoms approaching each other; (*upper curve*) antibonding state; (*lower curve*) bonding state; (*middle curve*) from free atom charge distribution bonding. Charge density distributions shown in the insert are for the two covalent states (after Kittel 1986 © John Wiley & Sons, Inc.)

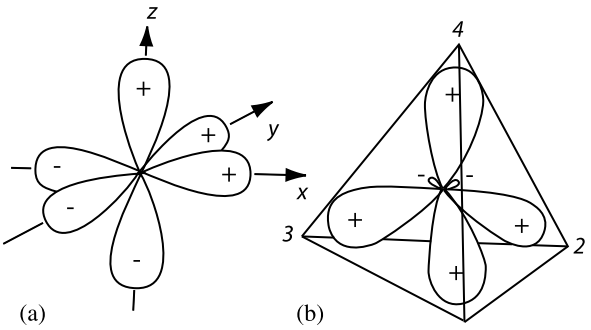

Fig. 1.7 Linear combination (hybridization) of a 1*s* function (spherical) with 3*p* functions (**a**) results in four sp^3 functions (**b**) which extend towards the four tetrahedra axes 1–4, and result in strongly directional bonding with a bond angle of 109.47°

Table 1.3 Bond lengths relevant to organic molecules α-Si and related semiconductors

Bond	Bond length (Å)	Bond	Bond length (Å)
C–C	1.54	Si–Si	2.35
C=C	1.38	Si–H	1.48
C=C	1.42 (graphite)	Ge–Ge	2.45
C≡C	1.21	Ge–H	1.55
C–H	1.09 (sp^3)	C–Si	1.87

(S) and the excited, anti-bonding state (A) shown. The figure also contains as center curve the classical contribution of two H-atoms with a charge density of free atoms: Such bonding is small compared with the covalent bonding shown in Table 1.3.

The bond length (center-to-center distance) between C-atoms in organic molecules decreases with increasing bonding valency as Other bond lengths typical for organic or similar molecules are also listed.

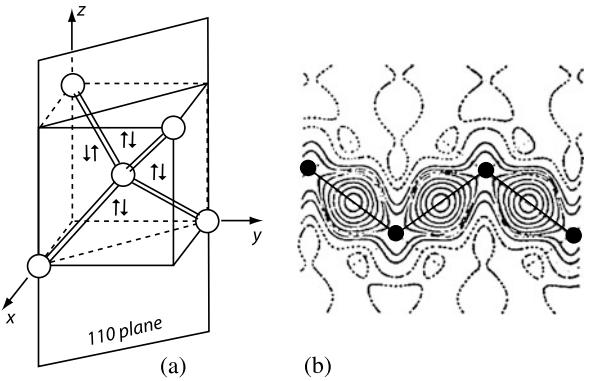

Fig. 1.8 (**a**) Unit cell of diamond with pairs of electrons indicated between adjacent atoms; (**b**) electron density profile within the (110) plane (after Dawson 1967)

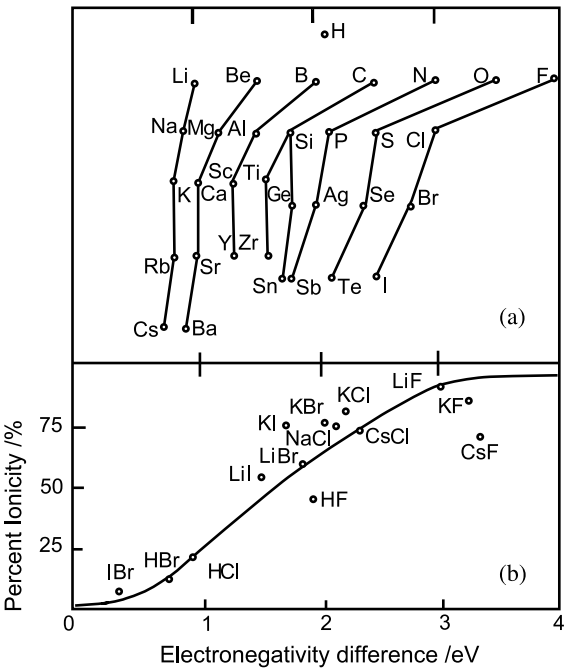

Fig. 1.9 (**a**) Electronegativity of the elements with groups from the periodic table of elements identified by interconnecting lines; (**b**) ionicity of alkali halides and halide molecules as a function of the difference in electronegativity (after Pauling 1960)

With additionally missing unpaired electrons in the outer shell, more than one atom of the same kind can be bound to each other. The number of bonded atoms is given by the following valency: monovalent atoms can form only diatomic molecules; divalent atoms, such as S or Se, can form chains; and trivalent atoms, such as As, can form two-dimensional (layered) lattices. Solids are formed from such elements by involving other bonding forces between the molecules, chains, or layers, e.g., van der Waals forces—see Sect. 1.5. Only tetravalent elements can form three-dimensional lattices which are covalently bound (e.g., Si).

1.2.1 Tetrahedrally Bound Elements

Silicon has four electrons in its outer shell. In the ground state of an isolated atom, two of the electrons occupy the s-state and two of them occupy p-states, with a $2s^2 2p^2$ configuration. By investing a certain amount of promotion energy,[3] this $s^2 p^2$-configuration is changed into an sp^3-configuration, in which an unpaired electron sits in each one of the singly occupied orbitals with tetrahedral geometry (see Fig. 1.7).

From the s-orbital and the three p-orbitals, four linear combinations can be formed, represented as $\sigma_i = 1/2(\varphi_s + \varphi_{px} \pm \varphi_{py} \pm \varphi_{pz})$, depending upon the choice of signs.

This is referred to as *hybridization*, with σ_i as the *hybrid function* responsible for bonding. When we bring together a large number of Si atoms, they arrange themselves so that each of them has four neighbors in tetrahedral geometry as shown in Fig. 1.9. Each atom then forms four electron bridges to its neighbors, in which each one is occupied with two electrons of opposite spin, as shown for the center atom in Fig. 1.8a. Such bridges become evident in a density profile within the (110) plane shown for two adjacent unit cells in Fig. 1.8b.

In contrast to the ionic bond, the covalent bond is angular-dependent, since the protruding atomic *eigenfunctions* extend in well-defined directions. Covalent bonding is therefore a *directional* and *saturable bonding*; the corresponding force is known as a *chemical valence force*, and acts in exactly as many directions as the valency describes.

1.3 Mixed Bonding

Crystals that are bonded partially by ionic and partially by covalent forces are referred to as *mixed-bond crystals*. Most semiconductors have a fraction of covalent and ionic bonding components (see, e.g., Mooser and Pearson 1956).

1.3.1 Tetrahedrally Bonded Binaries

By using the Grimm-Sommerfeld rule (see below) for isoelectronic rows of elements, Welker and Weiss (1954) predicted desirable semiconducting properties for III–V compounds.[4]

[3] The promotion energy is 4.3, 3.5, and 3.3 eV for C, Si, and α-Sn, respectively. However, when forming bonds by establishing electron bridges to neighboring atoms, a substantially larger energy is gained, therefore resulting in net binding forces. Diamond has the highest cohesive energy in this series, *despite* the fact that its promotion energy is the largest because its sp^3–sp^3 C–C bonds are the strongest (see Harrison 1980).

[4] Meaning compounds between one element of group III and one element of group V on the periodic system of elements.

Table 1.4 Static effective charges of partially covalent AB-compounds (after Coulson et al. 1962)

Compound	e^*/e	Compoud	e^*/e
ZnO	0.60	BN	0.43
		AlN	0.56
		GaN	0.55
		InN	0.58
ZnS	0.47	BP	0.32
CdS	0.49	AlP	0.46
HgS	0.46	GaP	0.45
		InP	0.49
ZnSe	0.47	AlAs	0.47
CdSe	0.49	GaAs	0.46
HgSe	0.46	InAs	0.49
ZnTe	0.45	AlSb	0.44
CdTe	0.47	GaSb	0.43
HgTe	0.49	InSb	0.46

Semiconducting III–V and II–VI compounds are bound in a *mixed bonding*, in which electron bridges exist, i.e., the bonding is directed, but the electron pair forming the bridge sits closer to the anion. This *degree of ionicity* increases for these compounds with an increased difference in electronegativity (Fig. 1.9) from III–V to I–VII compounds and within one class of compounds, e.g., from RbI to LiF—see also Table 1.4. The mixed bonding may be expressed as the sum of the wave functions describing covalent and ionic bonding

$$\psi = a\psi_{\text{cov}} + b\psi_{\text{ion}} \tag{1.8}$$

with the ratio b/a defining the *ionicity* of the bonding. This bonding can also be described as rapidly alternating between that of covalent and ionic. Over an average time period, a fraction of ionicity (b/a) results. The ionicity of the bonding can be described by a static *effective ion charge* $e^{\bullet}$, as opposed to a dynamic effective ion charge, which is less by a fraction on the order of b/a than in a purely ionic compound with the charge given by the valency.

The static effective charge for other II–VI and III–V compounds is given in Table 1.4.

The effective charge concept can be confusing if one does not clearly identify the ionic state of the system. For instance, in the case of CdS, a purely ionic state is $Cd^{++}S^{--}$, as opposed to the covalent state of $Cd^{--}S^{++}$ (which is equivalent to the $Si^x Si^x$-configuration). In other words, the covalent state is that in which both Cd and S have four valence electrons and are connected to each other by a double bond. This must not be confused with the neutral $Cd^x S^x$ configuration, which is a mixed-bonding state.

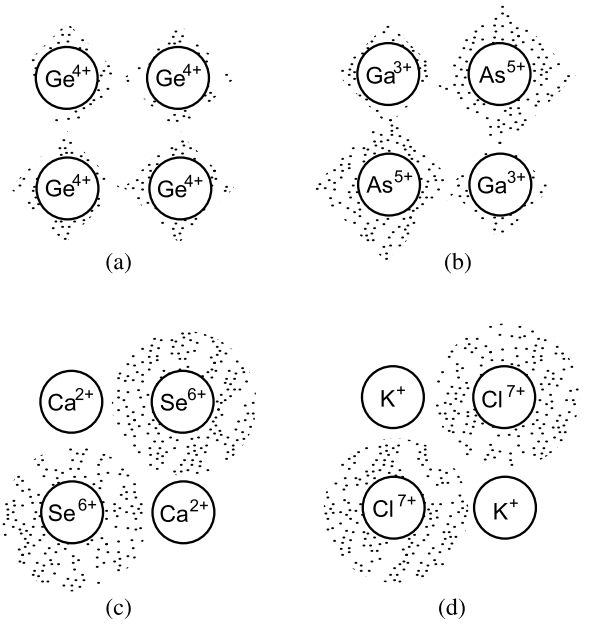

Fig. 1.10 Schematic sketch of mixed bonding from nearly perfect covalent (**a**) in Ge to perfect ionic (**d**) in KCl it shows diminishing bridge formation and increasing cloud formation of electrons around anions with increasing ionicity (after Ashcroft and Mermin 1976). For instance, in CdS the divalent behavior of Cd and S could result in a doubly charged $Cd^{++}S^{--}$ lattice, while measurements of the electric dipole moment indicate an effective charge of 0.49 for CdS

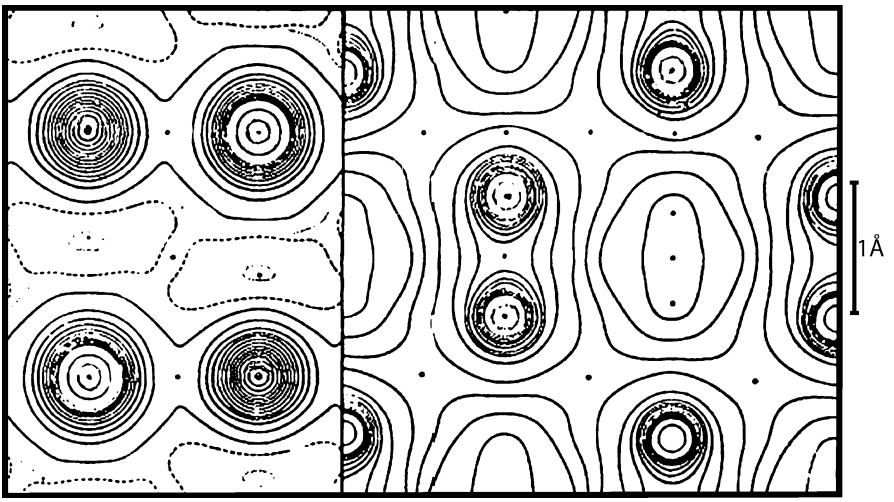

Fig. 1.11 Electron density distribution obtained by Fourier analysis of X-ray diffraction pattern of (**a**) NaCl and (**b**) diamond (after Brill et al. 1942)

The expression for the static effective charge (see Coulson et al. 1962) is

$$\frac{e^*}{e} = \frac{N(a/b)^2 - (8-N)}{1+(a/b)^2}, \tag{1.9}$$

Table 1.5 Ionic radii r_i and half the nearest-neighbor distances in metals r_m in Å (after Ashcroft and Mermin 1976)

Metal	r_i	r_m	r_m/r_i	Transition Metal	r_i	r_m	r_m/r_i
Li	0.60	1.51	2.52	Cu	0.96	1.28	1.33
Na	0.95	1.83	1.93	Ag	1.26	1.45	1.15
K	1.33	2.26	1.70	Au	1.37	1.44	1.05
Rb	1.48	2.42	1.64				
Cs	1.69	2.62	1.55				

with N as the valency. For $N = 2$, the effective charge vanishes when $a/b = \sqrt{3}$. For $N = 3$ in III–V compounds, e^* vanishes when $a/b = \sqrt{5}/3$, and for group IV semiconductors when $a = b$.

In crystals, low coordination numbers (typically 4) signify a considerable covalent contribution to the bonding.

The different degree of bridge formation in crystals with mixed bonding (Fig. 1.10) can be made visible by a Fourier analysis of X-ray diffraction from which the electron density distribution around each atom can be obtained. This is shown for a mostly ionic crystal in Fig 1.11a and for a mostly covalent crystal in Fig. 1.11b.

1.4 Metallic Bonding (Delocalized Bonding)

Metallic bonding can be understood as a collective interaction of a mobile electron fluid with metal ions. Metallic bonding occurs when the number of valence electrons is only a small fraction of the coordination number; then neither an ionic nor a covalent bond can be established.

Metallic bonding of simple metals, e.g., alkali metals, can be modeled by assuming that each metal atom has given up its valence electron, forming a lattice of positively charged ions, submerged in a fluid of electrons. Between the repulsive electron–electron and ion–ion interactions and the attractive electron-ion interaction, a net attractive binding energy results, which is *nondirectional and not saturable*, and results in *close-packed structures* with high coordination numbers (8 or 12; Wigner and Seitz 1933), but relatively wide spacing between the submerged metal ions (Table 1.5). Such metals have low binding energies ($\sim$1 eV/atom) and high compressibility. They are mechanically soft, since the nondirectional lattice-forces exert little resistance against plastic deformation. This makes metals attractive for forming and machining.

In other metals, such as transition group elements, the bonding may be described as due to covalent bonds which rapidly hop from atom pair to atom pair. Again, free electrons are engaged in this resonance-type bonding. These metals have a higher binding energy of $\sim$4 to 9 eV/atom and an interatomic distance that is closer to the one given by the sum of ionic radii (Table 1.5). They are substantially harder when

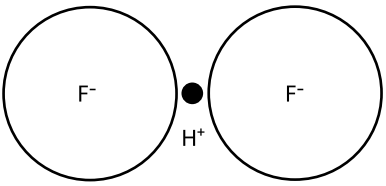

Fig. 1.12 Hydrogen bonding between a positive hydrogen ion (proton) and two ions (coordination number 2)

located in the middle of the transition metal row, e.g., Mo and W (Ashcroft and Mermin 1976).

In semiconductors with a very high density of free carriers, metallic binding forces may contribute a small fraction to the lattice bond, interfering with the predominant covalent bonding and usually weakening it, since these electrons are obtained by ionizing other bonds. Changes in the mechanical strength of the lattice can be observed in photoconductors in which a high density of free carriers can be created by light (Gorid'ko et al. 1961).

For more information, see Ziman (1969) and Harrison (1966).

1.5 Van der Waals Bonding

Noble gas atoms or molecules with saturated covalent bonds can be bound to each other by dipole-dipole interaction (Debye). The dipole is created between the nucleus (nuclei) of the atom (molecule) and the cloud of electrons moving around these nuclei, and forms a fluctuating dipole moment even for a spherically symmetrical atom. The interaction creates very weak, nonsaturable attractive forces. This results in low melting points and soft *molecule crystals*. The bonding energy can be approximated by

$$eV = -\frac{\alpha_a}{r^6} + \frac{\alpha_r}{r^{12}}. \tag{1.10}$$

Van der Waals forces are the main binding forces of organic semiconductors (van der Waals 1873).

1.6 Hydrogen Bonding

Hydrogen bonding (Fig. 1.12) is a type of ionic bonding in which the hydrogen atom has lost its electron to another atom of high electronegativity. The remaining proton establishes a strong Coulomb attraction. This force is not saturable. However, because of the small size of the proton, hydrogen bonding is strongly localized, and spatially no more than two ions have space to be attracted to it. When part of a molecule, the hydrogen bond—although ionic in nature—fixes the direction of the attached atom because of space consideration. It should not, however, be confused with the covalent bonding of hydrogen that occurs at dangling bonds in semiconductors, e.g., at the crystallite interfaces of polycrystalline Si or in amorphous Si:H.

1.7 Intermediate Valence Bonding

An interesting group of semiconductors are *transition metal com- pounds*. The transition metals have partially filled *inner* $3d$, $4d$, $5d$, or $4f$ shells and a filled outer shell that provides a shielding effect to the valence electrons. In these compounds the crystal field has a reduced effect. Some of these compounds show *intermediate valence bonding*. The resulting unusual properties range from resonant valence exchange transport in copper-oxide compounds (Anderson 1987; Anderson et al. 1987) to giant magnetoresistance and very large magneto-optical effects in rare-earth semiconductors. For a review, see Holtzberg et al. (1980).

1.8 Other Bonding Considerations

Other, more subtle bonding considerations have gained a great deal of interest because of their attractive properties. These are related to magnetic and special dielectric properties, to superconductivity, as well as to other exotic effects.

For instance, dilute semimagnetic semiconductors such as the alloy $Cd_{1-\varsigma}Mn_{\varsigma}Te$ (Furdnya 1982, 1986; Brandt and Moshchalkov 1984; Wei and Zunger 1986; Goede and Heitnbrodt 1988) show interesting magneto-optical properties. They change from paramagnetic ($\varsigma < 0.17$) to antiferromagnetic ($0.6 < \varsigma$) to the ferro- or antiferromagnetic behavior of MnTe; exhibit giant magneto-optical effects and bound magnetic polarons; and offer opportunities for optoelectric devices that are tunable by magnetic fields.

These materials favor specific structures and permit the existence of certain quasi-particles, such as small polarons or Frenkel excitons. These discussions require a substantial amount of understanding of the related physical effects, and are therefore postponed to a more appropriate section of this book (see also Phillips 1973; Harrison 1980; Ehrenreich 1987).

1.9 Atomic and Ionic Radii

The equilibrium distances between atoms in a crystal define atomic radii when assuming that hard-sphere atoms touching each other. In reality, however, these radii are soft with some variation of the electronic eigenfunctions and, for crystals with significant covalent fraction they depend on the angular atomic arrangement. However, for many crystals the hard-sphere radii are useful for most lattice estimates.

When comparing the lattice constants of chemically similar crystals, such as NaCl, NaBr, KCl, and KBr, one can determine the radii of the involved ions (Na^+, K^+, Cl^-, and Br^-) if at least one radius is known independently. Goldschmidt (1927) used the radii of F^- and O^{--} for calibration. Consequent listings of other ionic radii are therefore referred to as *Goldschmidt radii*. These radii are independent of the compound in which the atoms are incorporated as long as they exhibit

Table 1.6 Covalent (effective ionic charge $e^* = 0$) and standard ionic (identified by $\pm e^*$) radii in Å

e^*	+1	0		+2	0		+3	0
Li	0.68	1.34	Be	0.30	0.90	B	0.16	0.88
Na	0.98	1.54	Mg	0.65	1.30	Al	0.45	1.26
K	1.33	1.96	Ca	0.94	1.74	Sc	0.68	
Cu	0.96		Zn	0.74	1.31	Ga	0.62	1.26
Rb	1.48		Sr	1.10		Y	0.88	
Ag	1.26		Cd	0.97	1.48	In	0.81	1.44
Cs	1.67		Ba	1.2		La	1.04	
Au	1.37		Hg	1.10	1.48	Tl	0.95	1.47

	+4	0	−4		0	−3		0	−2
C		0.77	2.60	N	0.70	1.71	O	0.73	1.46
Si	0.38	1.17	2.71	P	1.10	2.12	S	1.04	1.90
Ti	0.60			As	1.18	2.22	Se	1.14	2.02
Ge	0.53	1.22	2.72						
Zn	1.77			Sb	1.36	2.45	Te	1.32	2.22
Sn		1.40	2.94						
Ce	0.92			Bi	1.46		Po		2.30
Pb	0.84	1.46							

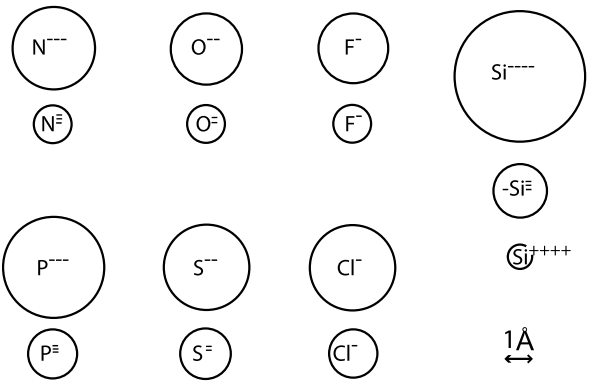

Fig. 1.13 Scale drawing of rigid sphere atoms with different bonding character (ionic or covalent, identified by the appropriate number of minus signs (*upper row*) or valence lines (*lower row*), respectively)

the same type of bonding. One distinguishes atomic, ionic, metallic, and van der Waals radii. Ionic radii vary with changing valency.

A list of the most important ion and atomic radii is given in Table 1.6. The drastic change in radii with changing bonding force (Mooser and Pearson 1956) is best demonstrated by comparing a few typical examples for some typical elements incorporated in semiconductors (Fig. 1.13). For more estimates of tetrahedral covalent radii, see van Vechten and Phillips (1970).

Table 1.7 Repulsive potential softness parameters (Eq. (1.3)) in Å (after Shanker and Kumar 1987)

Ion	r_0 (th)	r_0 (exp)	Ion	r_0 (th)	r_0 (exp)
Li^-	0.069	0.042	F^-	0.179	0.215
Na^+	0.079	0.090	Cl^-	0.238	0.224
K^+	0.106	0.108	Br^-	0.258	0.254
Rb^+	0.115	0.089	I^-	0.289	0.315
Cs^+	0.130	0.100			

Table 1.8 Change of interatomic distance Δ_m (in Å) for compounds deviating from coordination number $m = 6$

m	Δ_m	m	Δ_m	m	Δ_m	m	Δ_m
1	−0.50	4	−0.11	7	+0.04	10	+0.14
2	−0.31	5	−0.05	8	+0.08	11	+0.17
3	−0.19	6	0	9	+0.11	12	+0.19

The deviation from strict rigidity, i.e., the softness of the ionic spheres, is conventionally considered by using a softness parameter r_0 in the exponential repulsion formula [Eq. (1.3)]. This parameter is listed for a number of ions in Table 1.7.

This softness also results in a change of the standard ionic radii as a function of the number of surrounding atoms. A small correction Δ_m in the interionic distance is listed in Table 1.8. This needs to be considered when crystals with different coordination numbers m, i.e., the number of surrounding atoms, are compared with each other (e.g., CsCl and NaCl).

With increasing atomic number, the atomic (or ionic) radius of homologous elements increases. The cohesive force therefore decreases with increasing atomic (ionic) radii. Thus, compounds formed by the same bonding forces, and crystallizing with similar crystal structure, show a decrease, for example, in hardness,[5] melting point, and band gap, but an increase in dielectric constant and carrier mobility.

The ratio of ionic radii determines the preferred crystal structure of *ionic* compounds. This is caused by the fact that the energy gain of a crystal is increased with every additional atom that can be added per unit volume. When several possible atomic configurations are considered, the material crystallizes in a modification that maximizes the number of atoms in a given volume. This represents the state of lowest potential energy of the crystal, which is the most stable one. An elemental crystal with isotropic radial interatomic forces will therefore crystallize in a close-packed structure.

[5]This empirical quantity can be defined in several ways (e.g., as Mohs, Vickers, or Brinell *hardness*) and is a macroscopic mechanical representation of the cohesive strength of the lattice. In Table 1.9 the often used Mohs hardness is listed, which orders the listed minerals according to the ability of the higher-numbered one to scratch the lower-numbered minerals.

Table 1.9 Mohs hardness

Material	Chemistry	Lattice type	Hardness
Talc	$Mg_3H_2SiO_{12\cdot aq}$	Layer lattice	1
Gypsum	$CaSO_4{\cdot}H_2O$	Layer lattice	2
Iceland spar	$CaCO_3$	Layer lattice	3
Fluorite	CaF_2	Ion lattice	4
Apatite	$Ca_5F(PO_4)_3$	Ion lattice	5
Orthoclase	$KAlSi_3O_8$	SiO_4 frame	6
Quartz	SiO_2	SiO_4 frame	7
Topaz	$Al_2F_2SiO_4$	Mixed ion-valency lattice	8
Corundum	Al_20_3	Valency lattice	9
Diamond	C	Valency lattice	10

Table 1.10 Preferred lattice structure for AB-compounds with ionic binding forces (after Goldschmidt 1927)

r_A/r_B	Preferred stable lattice
<0.22	None
0.22...0.41	Zinc-blende or Wurtzite
0.41...0.72	NaCl lattice
>0.72	CsCl lattice

In a binary crystal, the ratio of atomic radii will influence the possible crystal structure. For isotropic nonsaturable interatomic forces, the resulting stable lattices are shown in Table 1.10 for different ratios of the ion radii.

When a substantial amount of covalent bonding forces are involved, the rules to select a stable crystal lattice for a given compound are more complex. Here atomic bond length and bond angles must be considered. Both can now be determined from basic principal density functions calculations. We can then define atomic radii from the turning point of the electron density distribution of each atom, and obtain an angular-dependent internal energy scale from these calculations (Zunger 1981). Using axes constructed from these radii, one obtains well-separated domains in which only one crystal structure is observed for binary compounds (Zunger 1981; Villars and Calvert 1985).

1.9.1 Bond-Length Relaxation in Alloys

The lattice constant of alloys $A_{1-\varsigma}B_{\varsigma}C$ of binary compounds AC and BC interpolates according to the concentration

$$a(\xi) = (1-\xi)a_{\mathrm{AC}} + \xi a_{\mathrm{BC}} \tag{1.11}$$

Table 1.11 Bond-length of isovalent impurity in given host lattice and bond-length relaxation parameter (after Martins and Zunger 1984)

System	$r_{BC}(AC:B)$ (Å)	ε	System	$r_{BC}(AC:B)$ (Å)	ε
AlP:In	2.480	0.65	InP:Al	2.414	0.73
GaP:In	2.474	0.63	InP:Ga	2.409	0.73
AlAs:In	2.653	0.60	InAs:Al	2.495	0.74
GaAs:In	2.556	0.62	InAs:Ga	2.495	0.73
AlSb:In	2.746	0.61	InSb:Al	2.693	0.75
GaSb:In	2.739	0.60	InSb:Ga	2.683	0.74
AlP:As	2.422	0.65	AlAs:P	2.395	0.67
AlP:Sb	2.542	0.61	AlSb:P	2.444	0.73
AlAs:Sb	2.574	0.60	AlSb:As	2.510	0.71
GaP:As	2.414	0.62	GaAs:P	2.387	0.68
GaP:Sb	2.519	0.57	GaSb:P	2.436	0.73
GaAs:Sb	2.564	0.60	GaSb:As	2.505	0.70
InP:As	2.595	0.67	InAs:P	2.562	0.74
InP:Sb	2.700	0.60	InSb:P	2.597	0.79
InAs:Sb	2.739	0.64	InSb:As	2.667	0.75
ZnS:Se	2.420	0.70	ZnSe:S	2.367	0.78
ZnS:Te	2.539	0.67	ZnTe:S	2.407	0.78
ZnSe:Te	2.584	0.71	ZnTe:Se	2.502	0.74
β-HgS:Se	2.611	0.76	HgSe:S	2.553	0.80
β-HgS:Te	2.716	0.71	HgTe:S	2.579	0.82
HgSe:Te	2.748	0.74	HgTe:Se	2.665	0.80
ZnS:Hg	2.482	0.73	β-HgS:Zn	2.380	0.80
ZnSe:Hg	2.587	0.74	HgSe:Zn	2.494	0.78
ZnTe:Cd	2.755	0.70	CdTe:Zn	2.674	0.78
ZnTe:Hg	2.748	0.69	HgTe:Zn	2.673	0.78
γ-CuCl:Br	2.440	0.81	γ-CuBr:Cl	2.367	0.79
γ-CuCl:I	2.563	0.80	γ-CuI:Cl	2.407	0.76
γ-CuBr:I	2.585	0.79	γ-CuI:Br	2.500	0.76
C:Si	1.665	0.35	Si:C	2.009	0.74
Si:Ge	2.380	0.58	Ge:Si	2.419	0.63
Si:Sn	2.473	0.53	α-Sn:Si	2.645	0.70
Ge:Sn	2.549	0.55	α-Sn:Ge	2.688	0.67

when they crystallize with the same crystal structure (Vegard 1921). However, the bond length between any of the three pairs of atoms is neither a constant, as suggested from the use of constant atomic radii (Pauling 1960), nor a linear interpolation as shown by the dotted line in Fig. 1.14 for total relaxation of the bond of atom B in a different chemical environment AC (or of A in BC).

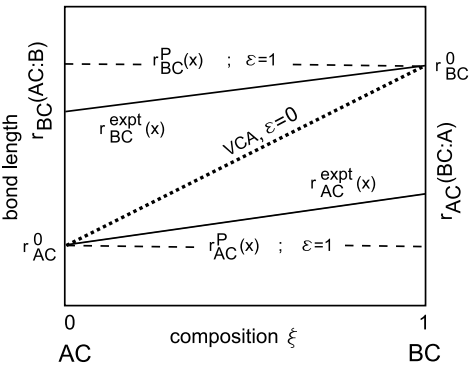

Fig. 1.14 Variation of bond-length in an $A_{1-\varsigma}B_{\varsigma}C$ alloy for rigid atoms ($\varepsilon = 1$), virtual crystal approximation ($\varepsilon = 0$), and experimentally observed relaxation

Table 1.12 Bond-length (d), bond-stretching (α) and bond-bending (β) force constants, calculated from elastic constants (after Martin 1970)

Crystal	d (Å)	α (N/m)	β (N/m)	Crystal	d (Å)	α (N/m)	β (N/m)
C	1.545	129.33	84.71	InP	2.541	43.04	6.24
Si	2.352	48.50	13.82	InAs	2.622	35.18	5.49
Ge	2.450	38.67	11.37	InSb	2.805	26.61	4.28
α-Sn	2.810	25.45	6.44	ZnS	2.342	44.92	4.81
SiC	1.888	88.	47.5	ZnSe	2.454	35.24	4.23
AlP	2.367	47.29	9.08	ZnTe	2.637	31.35	4.45
AlAs	2.451	43.05	9.86	CdTe	2.806	29.02	2.44
AlSb	2.656	35.35	6.79	β-HgS	2.534	41.33	2.56
GaP	2.360	47.32	10.46	HgSe	2.634	36.35	2.36
GaAs	2.448	41.19	8.94	HgTe	2.798	27.95	2.57
GaSb	2.640	33.16	7.23	γ-CuCl	2.341	22.9	1.01
				γ-CuBr	2.464	23.1	1.32
				γ-CuI	2.617	22.5	2.05

This nonrigidity of atoms is important when incorporating isovalent impurities into the lattice of a semiconductor (doping) and estimating the resulting deformation of the surrounding lattice. With the bond length r_{BC} within the AC lattice (see Table 1.11), one defines a relaxation parameter

$$\varepsilon = \frac{r_{BC}(AC:B) - r^0_{AC}}{r^0_{BC} - r^0_{AC}}. \tag{1.12}$$

The superscript 0 indicates the undisturbed pure crystal, the notation AC:B indicates B as doping element with a sufficiently small density incorporated in an AC compound, so that B–B interaction can be neglected.

This relaxation parameter can be estimated from the bond-stretching and bond-bending force constants α and β (see Table 1.12), according to Martins and Zunger (1984),

$$\varepsilon = \frac{1}{1 + \frac{1}{6}\frac{\alpha_{AC}}{\alpha_{BC}}[1 + 10\frac{\beta_{AC}}{\alpha_{AC}}]}, \tag{1.13}$$

yielding values of ε typically near 0.7—see Table 1.11; that is, isovalent impurity atoms behave more like rigid atoms ($\varepsilon = 1$) than totally relaxed atoms ($\varepsilon = 0$) in a virtual crystal approximation [Eq. (1.11)].

http://www.springer.com/978-3-642-36747-2

Handbook of the Physics of Thin-Film Solar Cells
Böer, K.W.
2013, XL, 882 p. 451 illus., Hardcover
ISBN: 978-3-642-36747-2